

# Effects of subsequent curing on chloride resistance and microstructure of steam-cured mortar

Yuquan Hu<sup>1a</sup>, Shaowei Hu<sup>\*2</sup>, Bokai Yang<sup>3</sup> and Siyao Wang<sup>4</sup>

<sup>1</sup>College of Civil and Transportation Engineering, Hohai University, 1 Xikang Road, Nanjing, China

<sup>2</sup>School of Civil Engineering, Chongqing University, 174 Shazheng Road, Chongqing, China

<sup>3</sup>The College of Mechanics and Materials, Hohai University, 8 Fucheng West Road, Nanjing, China

<sup>4</sup>School of Water Resources and Hydropower Engineering, Wuhan University, 8 Donghu South Road, Wuhan, China

(Received December 26, 2019, Revised March 24, 2020, Accepted March 30, 2020)

**Abstract.** The influence of subsequent curing on the performance of fly ash contained mortar under steam curing was studied. Mortar samples incorporated with different content (0%, 20%, 50% and 70%) of Class F fly ash under five typical subsequent curing conditions, including standard curing (ZS), water curing (ZW) under 25°C, oven-dry curing (ZD) under 60°C, frozen curing (ZF) under -10°C, and nature curing (ZN) exposed to outdoor environment were implemented. The unsteady chloride diffusion coefficient was measured by rapid chloride migration test (RCM) to analyze the influence of subsequent curing condition on the resistance to chloride penetration of fly ash contained mortar under steam curing. The compressive strength was measured to analyze the mechanical properties. Furthermore, the open porosity, mercury intrusion porosimetry (MIP), x-ray diffraction (XRD) and thermogravimetric analysis (TGA) were examined to investigate the pore characteristics and phase composition of mortar. The results indicate that the resistance to chloride ingress and compressive strength of steam-cured mortar decline with the increase of fly ash incorporated, regardless of the subsequent curing condition. Compared to ZS, ZD and ZF lead to poor resistance to chloride penetration, while ZW and ZN show better performance. Interestingly, under different fly ash contents, the declining order of compressive strength remains ZS>ZW>ZN>ZD>ZF. When the fly ash content is below 50%, the open porosity grows with increase of fly ash, regardless of the curing conditions are diverse. However, if the replacement amount of fly ash exceeds a certain high proportion (70%), the value of open porosity tends to decrease. Moreover, the main phase composition of the mortar hydration products is similar under different curing conditions, but the declining order of the C-S-H gels and ettringite content is ZS>ZD>ZF. The addition of fly ash could increase the amount of harmless pores at early age.

**Keywords:** steam-cured mortar; subsequent curing condition; fly ash; chloride resistance; microstructure

## 1. Introduction

The deterioration of reinforced concrete (RC) in aggressive environments is an important problem all over the world (Alexander and Beushausen 2019, Li *et al.* 2019). A lot of engineering accidents were reported for construction due to corrosion of reinforcing steel (Engineering.com 2018, Song *et al.* 2009, Pack *et al.* 2010). People commonly consider that chloride penetration is the main cause of steel corrosion and earlier failure for RC structure during service (Song *et al.* 2008, Tripathi 2012, Liu *et al.* 2014). Prestressed Concrete Cylinder Pipe (PCCP) as a kind of reinforced concrete structure would be inevitably employed in environments like coastal areas and saline-alkali lands containing many chlorides ions, which could penetrate into mortar cover and causes serious deterioration, such as loss of cross section of steel area (Noh and Sonoda 2016), loss of prestress and cover cracking (Chen *et al.* 2015). Noticeably, the performance of the mortar cover has a huge

impact on the ability to resist chloride ingress of RC structure. Relevant research has been carried out, for instance, the effect of curing methods, water to binder ratio, and mineral additive can be available from literature (Zou *et al.* 2018, Hosseini 2018, Monticelli *et al.* 2016).

Compared with standard curing, initial steam curing can accelerate the early hydration rate, achieve high early strength, provide the required strength level of concrete in a short time, and enhance the efficiency of mold turnover thus improving the production efficiency of products. Due to these outstanding advantages, steam curing has been widely applied in the manufacture of prefabricated components in recent years, for example, Prestressed Concrete Cylinder Pipe (PCCP) has been widely used in medium-long distance and heavy calibre water conveyance project. However, it is also reported that steam curing can lead to porosity increase and poor resistance to chloride ion penetration (Patel *et al.* 1995, Zou *et al.* 2019, Hooton and Titherington 2004). Not only that, the ultimate strengths of the heated treated concrete are lower than those of the standard cured specimens (Huang *et al.* 2019). In order to clarify the effect of steam curing on pore structure, Zou *et al.* (2019) investigated the multi-scale pore structure characteristics of concrete, paste and paste-aggregate interfacial zone during steam-curing process and reported that multi-scale pore

\*Corresponding author, Professor

E-mail: hushaowei@nhri.cn

<sup>a</sup>Ph.D. Student

E-mail: hhyuquan@163.com

Table 1 Chemical composition of cement and fly ash

Composition (by wet%).	OPC	Fly ash
Silica (SiO <sub>2</sub> )	19.64	49.37
Calcium oxide (CaO)	63.60	4.77
Magnesium oxide (MgO)	1.59	1.80
Iron Oxide (Fe <sub>2</sub> O <sub>3</sub> )	4.18	5.20
Alumina (Al <sub>2</sub> O <sub>3</sub> )	5.00	32.14
Potassium oxide (K <sub>2</sub> O)	0.81	1.59
Sulfur trioxide (SO <sub>3</sub> )	2.41	1.03
Sodium oxide (Na <sub>2</sub> O)	0.26	1.30
Loss on ignition	0.82	1.23

structure evolution of concrete is remarkably influenced by the steam curing process. Furthermore, a hydration degree-dependent and water to cement ratio-related theoretical model is established to characterize the pore structure evolution during steam-curing process. In order to lighten the adverse effect of steam curing on the reinforcement cover, some improvement measures including addition of supplementary cementitious materials, improvement of subsequent curing methods, optimization of steam curing and adding protective surface coatings were discussed in published literatures (Zou *et al.* 2018, Liu *et al.* 2005, Erdoğan and Kurbetçi 1998, Li *et al.* 2015).

Chloride resistance of concrete structures can be enhanced by replacing cement supplementary materials, which results in improvement in estimated service life of structures (Chai *et al.* 2011, Sengul and Tasdemir 2009). Verma *et al.* (2013) found that use of pozzolanic materials is more effective than decreasing the *W/C* ratio for improving the chloride resistance of concrete structures. Owing to the positive effects of energy conservation, economic and environment protection, fly ash has been widely adopted as cement replacement in cement-based materials (Kumar and Prasad 2019, Jena and Panda 2018, Kurtoğlu *et al.* 2018, Sahani *et al.* 2019). Meanwhile, the durability of composite material after adding fly ash is the key problem we need pay attention to (Zhang and Li 2013, Zhang and Li 2014). Jena and Panda (2015, 2017a, b, 2018, 2019) systematic reported the evaluation of mechanical properties and durability of blended concrete containing fly ash and silpozz. Three of the literatures specifically analyzed the influence of sea water on strength and durability properties of blended cement concrete (Jena and Panda 2015, 2017a, 2018). A number of literatures have indicated that incorporating of fly ash can effectively enhance the resistance of concrete to chloride penetration (Liu *et al.* 2017, Yang and Wang 2004, Siddique 2011, Baert and Poppe 2008, Ampadu *et al.* 1999). However, the influence of steam curing on the chloride resistance of fly ash contained mortar was not considered in the above studies. What's more, the influence of subsequent curing on the chloride ion migration resistance of fly ash contained mortar is rarely studied.

In this paper, a new insight is put forward to understand the effect of subsequent curing on the chloride resistance and microstructure of fly ash contained mortar after initial steam curing. Mortar specimen papered with 0%, 20%, 50% and 70% replacement ratios of fly ash were first exposed to

Table 2 Mixture proportions of mortar (kg/m<sup>3</sup>)

Sample	F0	F20	F50	F70
Cement	642	514	321	193
Fly ash	-	128	321	449
Sand	1478	1478	1478	1478
Water	244	244	244	244
Water reduce	1.2%	1.2%	1.2%	1.2%

initial steam curing and then subjected to five typical curing condition (standard curing, water curing, oven-dry curing, frozen curing and nature curing) over a period of up to 28 days. The purpose of selecting these subsequent curing regimes is to understand the effect of different typical service ambient conditions in china on the chloride resistance and microstructure of steam-cured mortar. The chloride diffusion coefficient was obtained by rapid chloride migration test (RCM) to characterize the effect of subsequent curing and replacement proportion of fly ash on the chloride resistance of steam-cured mortar. As we all known, there is a close relationship between the internal micropores and water absorption (Cullu and Arslan 2014). Hence, the open porosity was examined by a water absorptivity test. Moreover, the microstructure and phase composition of the mortar specimens were examined by mercury intrusion porosimetry (MIP), X-ray diffraction (XRD) and thermogravimetric analysis (TGA). Noteworthy, there is a close relationship between the compressive strength and permeability of mortar. Therefore, the compressive properties of mortar were also studied.

## 2. Materials and methods

### 2.1 Materials and specimen preparation

The cement used in this study was type P.O.42.5R Ordinary Portland Cement (OPC) provided by China Cement Plant (Nanjing) Co. Ltd. Class F fly ash was supplied by China Ningdong Power Plant. OPC and fly ash were detected by X Ray Fluorescence (XRF) to determine the chemical composition, as shown in Table 1. River sand was used as fine aggregate with the fitness modulus of 2.62 and the apparent density of 2628 kg/m<sup>3</sup>. A constant ratio of water to binder (*W/B*) was fixed at 0.38. Water reducer, produced by Qinfen (Shaanxi) Building Materials Co. Ltd, was added at rate of 1.2% to improve workability of mixture. These values are in accordance with the Chinese standard (JGJ52 2006).

Fly ash contained mortars with 0%, 20%, 50%, and 70% (by weight of OPC) fly ash replacement levels were fabricated. The mix design is targeted for M45 grade mortar and the mixture ratio of fly ash contained mortars are listed in Table 2. The cement, fly ash and sand were firstly putted into a forced single horizontal axis mortar mixer for 1 min dry-mixing. Then, running water and water reducer were slowly added and mixed for another 3 min. Finally, one part of the mortar mixture was cast into steel molds with a size of 100×100×100 mm to measure the compressive strength and open porosity, another part of mortar mixture was

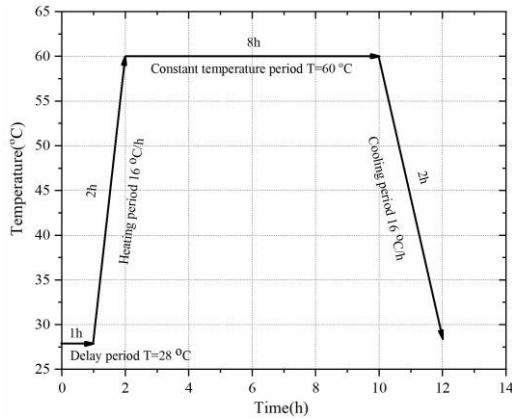


Fig. 1 Schematic of steam curing cycles used in this study

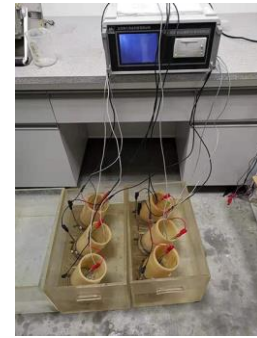
placed into PVC molds with a diameter of 100 mm and a height of 50 mm to quickly determine the unsteady chloride diffusion coefficient of mortar through the RCM test.

Fig. 1 shows the steam curing regime adopted in this study. The whole process lasted for 13 h with a delay period of 1 h, 2 h heating stage with rate of 16°C/h, 8 h constant temperature stage at 60°C and 2 h of cooling process with rate of 16°C/h (GB/T19685 2017, AWWAC301 2007). To examine the effect of subsequent curing on the early-age performance of steam-cured mortar, the steam-cured mortar samples were manufactured and divided into five groups for implementing different subsequent curing conditions, respectively. The following is the methods of subsequent curing methods: standard curing (ZS), water curing (ZW) under 25°C, oven-dry curing (ZD) under 60°C, frozen curing under -10°C (ZF), and nature curing (ZN) exposed to outdoor environment, whose temperature ranging from 25°C to 35°C and humidity is between 40% and 70%. Group ZW was used to simulate wet location in Southern China, where humidity is high and rainfall is abundant all the year round; Group ZD was selected to imitate the exceedingly dry and hot summer climate in Northwest China, where the land surface temperature can reach 60°C and little rainfall annual; Group ZF was used to characterize the winter environment in North China, where the average temperature in winter is about -10°C; Group ZN was chosen to represent the section of pipeline work exposed to the ground; Group ZS is laboratory environment as control group for comparison.

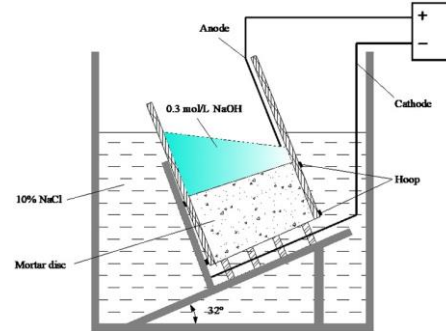
## 2.2 Testing methods

### 2.2.1 Rapid chloride migration test (RCM)

The test progress can be as follow JTS/T236 (2019). Fig. 2 shows the schematic diagram of the RCM test device. The actual thickness of sample was measured by a Vernier caliper. Two hoops were used to keep the flank of the sample in a sealed state. The anode chamber was immersed in 0.3 mol/L NaOH solution, and 10% NaCl solution was added in the cathode chamber. To remove air bubbles produced on the anode plate during the test, the platform was placed in an inclined position. The test ambient temperature was controlled at 25±2°C by an air conditioner. Power supply with variable voltage output 0-60 V was used.



(a) Photo of RCM test-up



(b)Details of RCM test-up

Fig. 2 RCM test device

Table 3 Duration ( $t$ ) of the RCM test, according to the initial current ( $I_0$ ) and voltage ( $U$ )

$I_0$ (mA)	$U$ (V)	Test current $I_i$ (mA)	Duration $t$ (h)
0-5	60	0-10	96
5-10	60	10-20	48
10-15	60	20-30	24
15-20	50	25-35	24
20-30	40	25-40	24
30-40	35	35-50	24
40-60	30	40-60	24
60-90	25	50-75	24
90-120	20	60-80	24

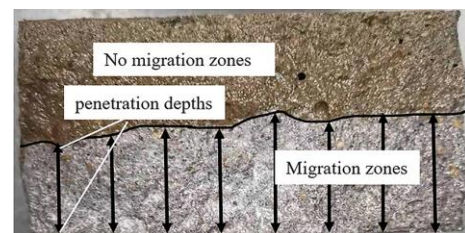


Fig. 3 Picture of chloride penetration depth based on spraying AgNO<sub>3</sub> solution indicator

The duration of RCM testing was determined based on the measured voltage and initial current, following Table 3. Besides, the initial and final temperature, the voltage and time was recorded, the chloride penetration depth inside a sample was determined by spraying 0.1 mol/L AgNO<sub>3</sub> solution on split sections and the area containing chloride ions appeared to be white and the average depth of ten points was considered as the result, as shown in Fig. 3. The chloride diffusion coefficient was calculated by Eq. (1)

(Nordtest NT Build 492 1999).

$$D_{RCM} = \left[ 0.0239(237 + T)L / (U - 2)t \right] \bullet \left[ X_d - 0.0238 \sqrt{(273 + T)LX_d / (U - 2)} \right] \quad (1)$$

where  $D_{RCM}$  denotes the non-steady-state chloride diffusion coefficient ( $m^2/s$ ),  $T$  refers to the average value of initial and final temperatures of anolyte ( $^{\circ}C$ ),  $L$  is the thickness of the mortar sample (mm),  $U$  is the value of voltage (V),  $X_d$  is the average value of penetration depths (mm), and  $t$  is the test duration (h).

### 2.2.2 Mechanical properties

As is known to all, the macro-performance of mortar is directly related to its compositions and microstructure, which is undoubtedly affected by the external curing condition. Therefore, according to JTS/T 236 (2019), the compressive strength of mortar was measured. To achieve reliable data, the average value of three samples in each group were taken as the results.

### 2.2.3 Open porosity

Firstly, the test mortar samples were dried to constant mass in an oven at  $105^{\circ}C$ . Then, all of the samples were immersed in water until constant mass and the final weight were recorded. Based on the test data, the open porosity can be calculated by the following formula

$$\eta = (m_s - m_d) / (V\rho_w) \quad (2)$$

where  $\eta$  is the open porosity,  $m_s$  is the mass of saturated sample,  $m_d$  is the mass of dried sample,  $V$  is the volume of sample,  $\rho_w$  is the density of water.

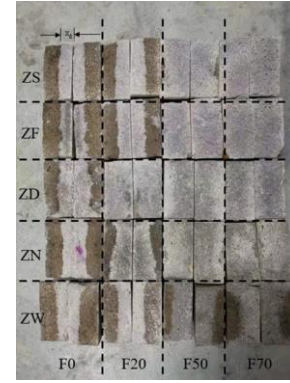
### 2.2.4 MIP, XRD and TGA

To make clear the distinct macro-properties of fly ash contained mortars under various subsequent curing conditions, part of the specimen was examined by microscopic methods, including mercury intrusion porosimetry (MIP), X-ray diffraction (XRD) and thermogravimetric analysis (TGA). The pore structure was evaluated with AutoPore IV 9500 V 1.09 mercury intrusion porosimeter (MIP). The measurable aperture was ranged from 1 nm to 100. During the measurement process, the pressure was between 0.2 and 35000 psia and the contact angle was  $140^{\circ}$ . The XRD patterns of paste were tested using a D8 Advance diffractometer with  $1.54 \text{ \AA}$  Cu  $K\alpha$  radiation, a scan speed of  $10^{\circ}$  per min from  $10^{\circ}$  to  $80^{\circ}$ . The measurement was operated at a voltage of 40 kV and current of 40 mA. TGA was performed on a 7 Synchronous Thermal Analyzer 449 F3 of NETZSCH. The analysis was operated under the atmosphere of nitrogen with a heating rate of  $10^{\circ}C / \text{min}$  from  $30^{\circ}C$  to  $1000^{\circ}C$ .

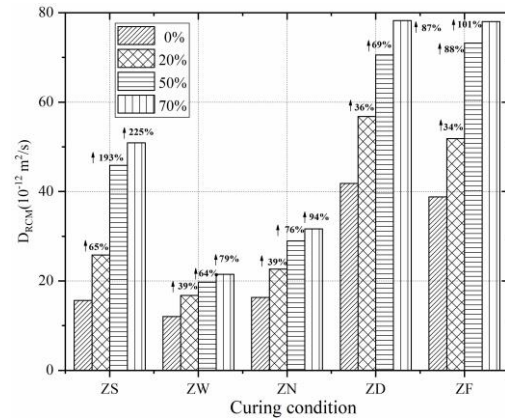
## 3. Results and discussion

### 3.1 The chloride diffusion coefficient of the mortar samples by RCM test

Compared with the long-term soaking method, the rapid chloride migration (RCM) test method is a fast, reliable,



(a) Photos after chloride penetration



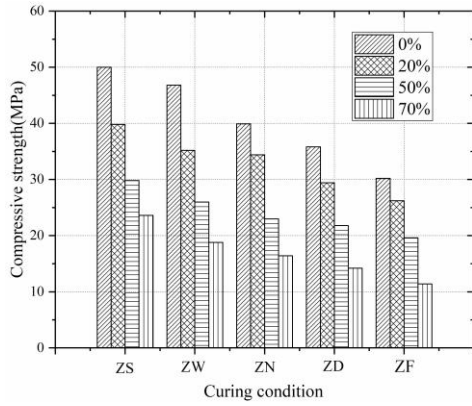
(b) The values of  $D_{RCM}$

Fig. 4 Results of RCM test

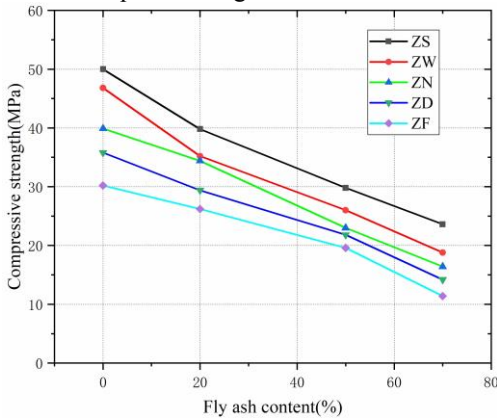
and effective way for measuring the unsteady chloride migration coefficient of concrete with different types of supplementary cementitious materials (Shi 2004, Spiesz and Brouwers 2012). Therefore, in this study, the unsteady rapid chloride migration coefficient was measured at 28 days by RCM to indicate early-age chloride resistance of fly ash contained mortar.

After the RCM test, the chloride penetration states are shown in Fig. 4(a) and the chloride migration coefficient ( $D_{RCM}$ ) was calculated by Eq. (1). The values and incremental percentages relative to no fly ash of  $D_{RCM}$  are shown in Fig. 4(b). It is conspicuously found a sharp increase of  $D_{RCM}$  in high volume fly ash contained mortar (50% and 70%). The  $D_{RCM}$  grow with the increase of fly ash content, regardless of subsequent curing conditions. The reason can be explained that the fly ash incorporated in mortar can result in reduced cement component, which decays the cement hydration reaction and produces a few C-S-H (calcium silicate hydrates) at early curing ages. Therefore, the large capillary pore size cannot be filled up and results in the resistance to chloride ingress weakened. Noteworthy, in the case of the same replacement amount of fly ash, steam-cured mortar under water curing and nature curing show better resistance to chloride penetration compared to standard curing at early curing ages. On the contrary, oven-dry curing and frozen curing lead to poor chloride resistance.

From discussion above, it would be reasonable to have faith in that there is a significant influence between the



(a) The compressive strength of mortar samples under different subsequent curing conditions



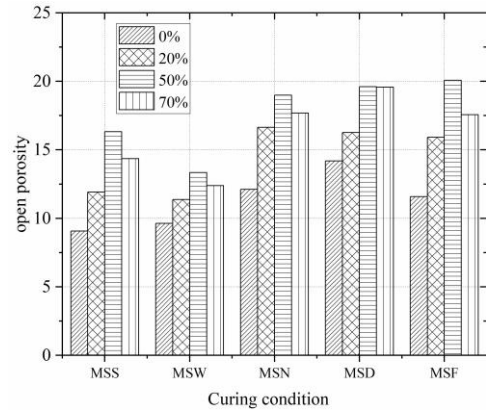
(b) The compressive strength of mortar samples with different fly ash contents

Fig. 5 The compressive strength of mortar samples

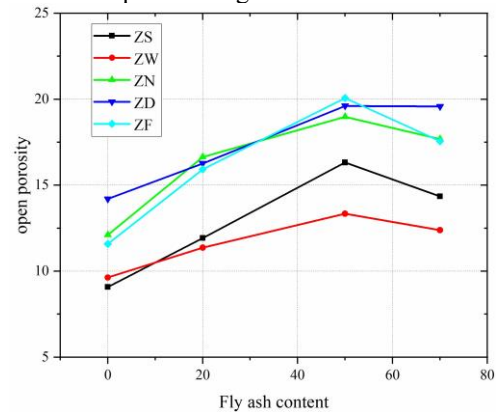
amount of fly ash incorporated in and subsequent curing condition on chloride resistance of steam-cured mortars. As is known to all, the resistance to chloride ingress of cementitious composition is not only closely associated with its macro-mechanical properties, for example, compressive strength, but also related to its microstructure and phase composition, such as porosity, pore structure and hydration products, which will be discussed in more detail below.

### 3.2 Compressive strength

The compressive strength mortar samples containing various contents of fly ash under various subsequent curing conditions is shown in Fig. 5. It can be easily found in Fig. 5 that the compressive strength declines with the increase of fly ash incorporated in mortar, regardless of the curing process, which in accordance with the law of  $D_{RCM}$ . Reduction for compressive strength were nearly 50% for mortar containing contents of fly ash by 70%. It's worth nothing that according to RCM test results, subsequent water curing and nature curing show better resistance to chloride ingress than standard curing, while the standard curing get the highest compressive strength, which means that the relationship between compressive strength and chloride resistance is complex. Moreover, only strength of subsequent standard curing and water curing mortar without



(a) The open porosity of mortar samples under different subsequent curing conditions



(b) The open porosity of mortar samples with different fly ash contents

Fig. 6 The open porosity of mortar samples

fly ash incorporated is higher than 45 MPa which meets the design strength. The nature curing, oven-dry curing and frozen curing resulted in reduction in compressive strength for all fly ash contents contained of mortar specimen. The reason is that there is insufficient water in the hydration process.

As cement based material, cement hydration has extremely important influence on the compressive strength of mortar, which is similar to concrete. Therefore, the research on the influence of hydration reaction on concrete compressive strength can be used as a reference. Neville (1995) reported that at least 80% relative humidity is necessary for the progress of hydration. Due to the decrease of water and part of the liquid phase water is converted into ice, hydration is not completed, leading to compressive strength reduction of nature curing and dry curing. Similar to Türkmen and Kantarcı (2007) reported that the lime-saturated cured samples give higher compressive strength than dry cured samples of concrete. Significantly, the lowest strength of frozen curing is also related to that the higher frost heaving force makes the pores coarser due to the higher ice content in steam-cured mortar.

### 3.3 Open porosity

Based on Eq. (2), the change law of open porosity under distinct curing conditions is shown in Fig. 6.

Table 4 Pore structure of mortar containing various fly ash under different curing modes

Group	Total pore volum/(ml·g <sup>-1</sup> )	Pore diameter ratio/ (%)			
		<20 nm	20-50 nm	50-200 nm	>200 nm
ZS-0	0.0538	10.55	13.03	64.05	12.37
ZS-50	0.0851	15.49	20.36	53.92	10.23
ZD-0	0.0689	6.44	9.12	69.28	15.16
ZF-0	0.0742	5.87	6.98	68.98	18.17

When the fly ash contents are blow 50%, the open porosity grows with increase of fly ash, regardless of the curing conditions are diverse, which is similar to chloride diffusion coefficient and compressive strength. However, the difference is that when the replacement amount of fly ash exceeds a certain high proportion (70%), the value of open porosity tends to decrease. It is inferred that steam curing can intensify the early hydration reaction of cement, lead to the evacuation of internal structure. Therefore, if the cement is extensive replaced by fly ash, the intensity of early cement hydration reaction will be weakened, and thus the opening porosity will be diminished. Furthermore, the group of ZS and ZW mortar indicate low open porosity also prove Neville's (1995) findings.

### 3.4 Mercury intrusion porosimetry (MIP)

The chloride resistance of cement-based materials is not only related to porosity, but also to pore structure (Scrivener 2004). Wu (1979) investigated the impact of pore structure on properties of cementitious material and reported that the pore in concrete can be classified as harmless pore (smaller than 20 nm), less-harmful pore (between 20 and 50 nm), harmful pore (between 50 and 200 nm) and more-harmful pore (bigger than 200 nm) (Mei *et al.* 2018). In this study, the pore structure is characterized with MIP, as shown in Table.4.

It is obvious that compared to ZS-0 sample, both ZD-0 and ZF-0 present an evident increase in total pore volume, which corresponding to the results of chloride diffusion coefficient, compressive strength and open porosity. Furthermore, it is easy to find that the addition of fly ash could increase the amount of harmless pores, which confirms the formal analysis that the cement hydration reaction was declined due to cement is largely replaced by fly ash. Noteworthy, for mortars whether added fly ash or not and no matter what subsequent curing mode was adopted, the amount of harmful pores (50-200 nm) accounts for the highest proportion and the ratio of more-harmful pores (>10%) is relatively high than standard curing specimens (Mei *et al.* 2018). The possible reasons may include the following aspects: the water migration inside cement-based materials can be accelerated by high temperature, resulting in numerous connecting holes (Ba *et al.* 2011, Geng *et al.* 2011). Moreover, despite high temperature can promote the hydration process of cementitious materials, the products of crystallization hydration are usually large in volume, unevenly distributed and easy to form more pores. In this case, the

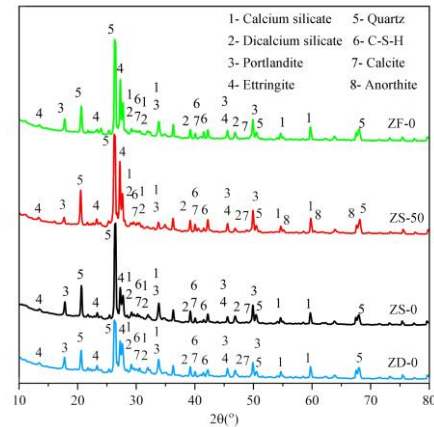


Fig. 7 XRD patterns of the mortar samples

highest ratios of harmful pores and more-harmful pores can be found.

### 3.5 X-ray diffraction (XRD)

XRD patterns of the mortar samples with different amount of fly ash incorporated in under different curing conditions is shown in Fig. 7. According to XRD patterns of ZS-0, ZF-0 and ZD-0, it is obvious that the main phase composition of the mortar hydration products is similar under different curing conditions. For all samples, quartz and portlandite and were the major crystalline hydration products. This result indicates that the curing conditions in this paper cannot change the phase composition of hydration products. However, the declining order of the peaks of C-S-H gels ( $42.16^\circ 2\theta$ ) is ZS-0>ZF-0>ZD-0, which indicates that the curing conditions can affect the content of hydration products. In addition, compared with the sample ZS-0, ZS-50 had lower peaks of portlandite ( $33.82^\circ 2\theta$ ) and anorthite related fly ash was found, which confirms that fly ash can affect the hydration process of mortar. It is known that the content of C-S-H, portlandite and other hydration products in cementitious material plays an important role in chloride resistance. In order to distinguish the content of hydration products, further analysis by TGA is needed.

### 3.6 Thermogravimetric analysis (TGA)

Fig. 8 presents TG and TGA curves of different amount of fly ash incorporated in mortar samples under distinct subsequent curing condition. Several obvious peaks in DTG curves can be observed. The first peak existing between  $85^\circ\text{C}$  and  $100^\circ\text{C}$  represents the dehydration of C-S-H gels (Saca and Georgescu 2014). The ettringite peak occurring between  $120^\circ\text{C}$  and  $140^\circ\text{C}$  (Yan *et al.* 2019). The portlandite ( $\text{Ca}(\text{OH})_2$ ) decompose into calcium oxide and water at about  $430^\circ\text{C}$ . In addition, the final peak at about  $630^\circ\text{C}$  was attributed to the decomposition of calcite into calcium oxide and carbon dioxide (Yan *et al.* 2019).

It is noteworthy that the mortar with 50% replacement of fly ash after ZS curing had much lower contents of ettringite, C-S-H gels, portlandite and calcite than that of no

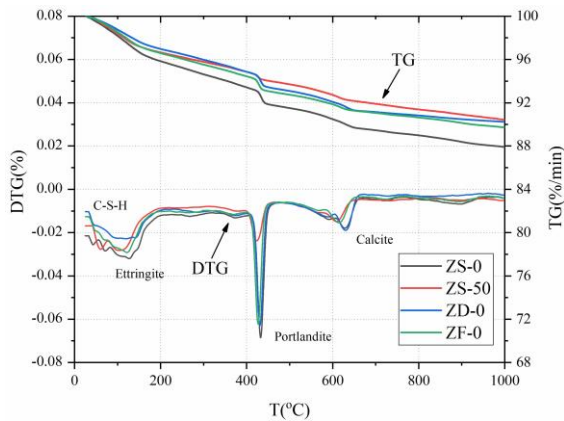


Fig. 8 TG, DTG curves of mortar samples

fly ash contained mortar test piece. This demonstrates the fact mentioned in RCM test results that the fly ash replacement decays the early cement hydration and produces a few C-S-H. The subsequent curing methods also has important impact on the production of hydration reaction. Obviously, the content of C-S-H gel and ettringite in the mortar after ZD curing was the lowest, followed by the test pieces after ZF curing, and the content of C-S-H gel and ettringite in the mortar after ZS curing was the highest. The findings can be used to prove the results of RCM tests and open porosity that the capillary pore size can be filled by C-S-H gels and thus the resistance to chloride ingress of ZS curing mortar will be enhanced. However, this observation seems to be a contradiction with the findings that ZD curing has higher open porosity than ZF curing. It can be explained that ZF has larger connected pores, which may lead to dissolution of C-S-H gels and portlandite in mortar. Remarkably, early steam curing not only makes the pore distribution of hydration products more extensive, but also diminishes the stability of hydration products, leading to the hydration products more easily dissolved.

#### 4. Conclusions

Based on the current experimental results, the main conclusion can be stated as follows:

- The resistance to chloride penetration and compressive strength of steam-cured mortar measured at 28 days decline with the increase of fly ash content, regardless of the subsequent curing conditions are diverse. Compared with subsequent standard curing, the subsequent water curing and nature curing show better resistance to chloride resistance while dry curing and frozen curing lead to poorer chloride resistance at 28 days curing ages.
- Under different fly ash contents, the declining order of mortar compressive strength remains ZS>ZW>ZN>ZD>ZF. When the fly ash content is below 50%, the open porosity grows with increase of fly ash, regardless of the curing conditions are diverse. However, if the replacement amount of fly ash attains to 70 %, the value of open porosity tends to decrease.
- For samples whether added fly ash or not and no

matter what subsequent curing mode was adopted, the amount of harmful pores (50-200 nm) accounts for the highest proportion. Besides, the ratio of more-harmful pores is relatively high (>10%) than standard curing specimens. This also demonstrates that heat damage effect of initial steam curing proposed in previous studies further.

- The subsequent curing condition and fly ash contents have significant influence on the production of hydration reaction. The main phase composition of the mortar hydration products is similar under different curing conditions. However, the declining order of the C-S-H gels and ettringite content is ZS>ZD>ZF. The reason that ZD curing has higher open porosity than ZF curing can be explained that ZF has larger and interconnected pores, which may lead the dissolving out of C-S-H gels and portlandite in mortar.

#### Acknowledgments

This research is supported by the National Key Research and Development Program of China (grant no. 2016YFC0401902). The authors also acknowledge the financial supports for this research from the National Natural Science Foundation of China (grant no. 51739008, 51527811).

#### References

- Alexander, M. and Beushausen, H. (2019), "Durability, service life prediction, and modelling for reinforced concrete structures-review and critique", *Cement Concrete Res.*, **122**, 17-29. <https://doi.org/10.1016/j.cemconres.2019.04.018>.
- Ampadu, K.O., Torii, K. and Kawamura, M. (1999), "Beneficial effect of fly ash on chloride diffusivity of hardened cement paste", *Cement Concrete Res.*, **29**(4), 585-590. [https://doi.org/10.1016/S0008-8846\(99\)00047-2](https://doi.org/10.1016/S0008-8846(99)00047-2).
- AWWA C301 (2007), Prestressed Concrete Pressure Pipe, Steel-Cylinder Type, American Water Works Association, American National Standard Institute; Denver, USA.
- Ba, M.F., Qian, C.X., Guo, X.J. and Han, X.Y. (2011), "Effects of steam curing on strength and porous structure of concrete with low water/binder ratio", *Constr. Build. Mater.*, **25**(1), 123-128. <https://doi.org/10.1016/j.conbuildmat.2010.06.049>.
- Baert, G., Poppe, A.M. and Belie, N.D. (2008), "Strength and durability of high-volume fly ash concrete", *Struct. Concrete*, **9**(2), 101-108. <https://doi.org/10.1680/stco.2008.9.2.101>.
- Chai, W., Li, W. and Ba, H. (2011), "Experimental study on predicting service life of concrete in the marine environment", *Open Civil Eng. J.*, **5**, 93-99. <https://doi.org/10.2174/1876523801104010093>.
- Chen, E. and Leung, C.K. (2015), "Finite element modeling of concrete cover cracking due to non-uniform steel corrosion", *Eng. Fract. Mech.*, **134**, 61-78. <https://doi.org/10.1016/j.engfracmech.2014.12.011>.
- Çullu, M. and Arslan, M. (2014), "The effects of chemical attacks on physical and mechanical properties of concrete produced under cold weather conditions", *Constr. Build. Mater.*, **57**, 53-60. <https://doi.org/10.1016/j.conbuildmat.2014.01.072>.
- Engineering.com (2018), Italy's Morandi Bridge Collapse-What Do We Know?, Deutsch.
- Erdoğan, S. and Kurbetci, S. (1998), "Optimum heat treatment

- cycle for cements of different type and composition”, *Cement Concrete Res.*, **28**(11), 1595-1604. [https://doi.org/10.1016/S0008-8846\(98\)00134-3](https://doi.org/10.1016/S0008-8846(98)00134-3).
- GB/T 19685 (2017), *Prestressed Concrete Cylinder Pipe*, China Standard Press, Beijing, China.
- Geng, J., Peng, B. and Sun, J.Y. (2011), “Effect of steam curing system on pore structure of cement paste”, *J. Build. Mater.*, **14**(1), 116-118. (in Chinese)
- Hooton, R.D. and Titherington, M.P. (2004), “Chloride resistance of high-performance concretes subjected to accelerated curing”, *Cement Concrete Res.*, **34**(9), 1561-1567. <https://doi.org/10.1016/j.cemconres.2004.03.024>.
- Hosseini, S.A. (2018), “Experimental study of the effect of water to cement ratio on mechanical and durability properties of Nano-silica concretes with Polypropylene fibers”, *Sci. Iran*, **26**(5), 2712-2722. <https://doi.org/10.24200/SCI.2017.5077.1079>.
- Huang, X., Hu, S., Wang, F., Yang, L., Rao, M., Mu, Y. and Wang, C. (2019), “The effect of supplementary cementitious materials on the permeability of chloride in steam cured high-ferrite Portland cement concrete”, *Constr. Build. Mater.*, **197**, 99-106. <https://doi.org/10.1016/j.conbuildmat.2018.11.107>.
- Jena, T. and Panda, K.C. (2015), “Influence of sea water on strength and durability properties of concrete”, *Adv. Struct. Eng.*, **03**, 1863-1873. [https://doi.org/10.1007/978-81-322-2187-6\\_143](https://doi.org/10.1007/978-81-322-2187-6_143).
- Jena, T. and Panda, K.C. (2017a), “Compressive strength and carbonation of sea water cured blended concrete”, *Int. J. Civil Eng. Technol.*, **8**(2), 153-162.
- Jena, T. and Panda, K.C. (2017b), “Usage of fly ash and silpozz on strength and surpitivity of marine concrete”, *Int. J. Appl. Eng. Res.*, **12**(16), 5768-5780.
- Jena, T. and Panda, K.C. (2018), “Mechanical and durability properties of marine concrete using fly ash and silpozz”, *Adv. Concrete Constr.*, **6**(1), 47-68. <https://doi.org/10.12989/acc.2018.6.1.047>.
- Jena, T. and Panda, K.C. (2019), “Study on strength reduction factor of blended concrete exposed to sea water”, *Rec. Adv. Struct. Eng.*, **1**, 787-801. [https://doi.org/10.1007/978-981-13-0362-3\\_64](https://doi.org/10.1007/978-981-13-0362-3_64).
- JGJ 52 (2006), *Standard for Technical Requirements and Test Method of Sand and Crushed Stone (or Gravel) for Ordinary Concrete*, China Construction Industry Press, Beijing, China.
- JTS/T 236 (2019), *Technical Specification for Concrete Test and Detection of Water Transport Engineering*, People’s Communications Press Co., Ltd.; Beijing, China.
- Kumar, V.P. and Prasad, D.R. (2019), “Influence of supplementary cementitious materials on strength and durability characteristics of concrete”, *Adv. Concrete Constr.*, **7**(2), 75-85. <https://doi.org/10.12989/acc.2019.7.2.075>.
- Kurtoğlu, A.E., Alzebaree, R., Aljumaili, O. and Nis, A. (2018), “Mechanical and durability properties of fly ash and slag based geopolymer concrete”, *Adv. Concrete Constr.*, **6**(4), 345-362. <https://doi.org/10.12989/acc.2018.6.4.345>.
- Li, G., Yang, B.Y., Guo, C.S., Du, J.M. and Wu, X.S. (2015), “Time dependence and service life prediction of chloride resistance of concrete coatings”, *Constr. Build. Mater.*, **83**, 19-25. <https://doi.org/10.1016/j.conbuildmat.2015.03.003>.
- Li, K., Zhang, D., Li, Q. and Fan, Z. (2019), “Durability for concrete structures in marine environments of HZM project: Design, assessment and beyond”, *Cement Concrete Res.*, **115**, 545-558. <https://doi.org/10.1016/j.cemconres.2018.08.006>.
- Liu, B., Xie, Y. and Li, J. (2005), “Influence of steam curing on the compressive strength of concrete containing supplementary cementing materials”, *Cement Concrete Res.*, **35**(5), 994-998. <https://doi.org/10.1016/j.cemconres.2004.05.044>.
- Liu, J., Tang, K., Qiu, Q., Pan, D., Lei, Z. and Xing, F. (2014), “Experimental investigation on pore structure characterization of concrete exposed to water and chlorides”, *Mater.*, **7**, 6646-6659. <https://doi.org/10.3390/ma7096646>.
- Liu, J., Wang, X., Qiu, Q., Ou, G. and Xing, F. (2017), “Understanding the effect of curing age on the chloride resistance of fly ash blended concrete by rapid chloride migration test”, *Mater. Chem. Phys.*, **196**, 315-323. <https://doi.org/10.1016/j.matchemphys.2017.05.011>.
- Mei, J., Ma, B., Tan, H., Li, H., Liu, X., Jiang, W., Zhang, T. and Guo, Y. (2018), “Influence of steam curing and nano silica on hydration and microstructure characteristics of high volume fly ash cement system”, *Constr. Build. Mater.*, **171**, 83-95. <https://doi.org/10.1016/j.conbuildmat.2018.03.056>.
- Monticelli, C., Natali, M.E., Balbo, A., Chiavari, C., Zanotto, F., Manzi, S., and Bignozzi, M.C. (2016), “A study on the corrosion of reinforcing bars in alkali-activated fly ash mortars under wet and dry exposures to chloride solutions”, *Cement Concrete Res.*, **87**, 53-63. <https://doi.org/10.1016/j.cemconres.2016.05.010>.
- Neville, A.M. (2011), *Properties of Concrete*, Copyright Licensing Agency Ltd, London, United Kingdom.
- Noh, H.M. and Sonoda, Y. (2016), “Potential effects of corrosion damage on the performance of reinforced concrete member”, *MATEC Web of Conferences*, **47**, 02007. <https://doi.org/10.1051/mateconf/20164702007>.
- NT Build 492 (2019), *Concrete, Mortar, and Cement-Based Repair Materials: Chloride Migration Coefficient from Non-Steady-State Migration Experiments*, Nordtest, Espoo, Finland.
- Pack, S.W., Jung, M.S., Song, H.W. and Kim, S.H. (2010), “Prediction of time dependent chloride transport in concrete structures exposed to a marine environment”, *Cement Concrete Res.*, **40**(2), 302-312. <https://doi.org/10.1016/j.cemconres.2009.09.023>.
- Panda, K.C. and Prusty, S.D. (2015), “Influence of silpozz and rice husk ash on enhancement of concrete strength”, *Adv. Concrete Constr.*, **3**(3), 203-221. <https://doi.org/10.12989/acc.2015.3.3.203>.
- Patel, H.H., Bland, C.H. and Poole, A.B. (1995), “The microstructure of concrete cured at elevated temperatures”, *Cement Concrete Res.*, **25**(3), 485-490. [https://doi.org/10.1016/0008-8846\(95\)00036-C](https://doi.org/10.1016/0008-8846(95)00036-C).
- Saca, N. and Georgescu, M. (2014), “Behavior of ternary blended cements containing limestone filler and fly ash in magnesium sulfate solution at low temperature”, *Constr. Build. Mater.*, **71**, 246-253. <https://doi.org/10.1016/j.conbuildmat.2014.08.037>.
- Sahani, A.K., Samanta, A.K. and Roy, D.K.S. (2019), “Influence of mineral by-products on compressive strength and microstructure of concrete at high temperature”, *Adv. Concr. Constr.*, **7**(4), 263-275. <https://doi.org/10.12989/acc.2019.7.4.263>.
- Scrivener, K.L. (2004), “Backscattered electron imaging of cementitious microstructures: understanding and quantification”, *Cement Concrete Compos.*, **26**(8), 935-945. <https://doi.org/10.1016/j.cemconcomp.2004.02.029>.
- Sengul, O. and Tasdemir, M.A. (2009), “Compressive strength and rapid chloride permeability of concretes with ground fly ash and slag”, *J. Mater. Civil Eng.*, **21**(9), 494-501. [https://doi.org/10.1061/\(ASCE\)0899-1561\(2009\)21:9\(494\)](https://doi.org/10.1061/(ASCE)0899-1561(2009)21:9(494)).
- Shi, C. (2004), “Effect of mixing proportions of concrete on its electrical conductivity and the rapid chloride permeability test (ASTM C1202 or ASSHTO T277) results”, *Cement Concrete Res.*, **34**, 537-545. <https://doi.org/10.1016/j.cemconres.2003.09.007>.
- Siddique, R. (2011), “Properties of self-compacting concrete containing class F fly ash”, *Mater. Des.*, **32**(3), 1501-1507. <https://doi.org/10.1016/j.matdes.2010.08.043>.
- Song, H.W., Lee, C.H. and Ann, K.Y. (2008), “Factors influencing chloride transport in concrete structures exposed to marine environments”, *Cement Concrete Compos.*, **30**(2), 113-121. <https://doi.org/10.1016/j.cemconcomp.2007.09.005>.
- Song, H.W., Pack, S.W. and Ann, K.Y. (2009), “Probabilistic

- assessment to predict the time to corrosion of steel in reinforced concrete tunnel box exposed to sea water”, *Constr. Build. Mater.*, **23**(10), 3270-3278. <https://doi.org/10.1016/j.conbuildmat.2009.05.007>.
- Spiesz, P. and Brouwers, H.J.H. (2012), “Influence of the applied voltage on the rapid chloride migration (RCM) test”, *Cement Concrete Res.*, **42**(8), 1072-1082. <https://doi.org/10.1016/j.cemconres.2012.04.007>.
- Tripathi, S.R., Ogura, H., Inoue, H., Hasegawa, T., Takeya, K. and Kawase, K. (2012), “Measurement of chloride ion concentration in concrete structures using terahertz time domain spectroscopy (THz-TDS)”, *Corros. Sci.*, **62**, 5-10. <https://doi.org/10.1016/j.corsci.2012.05.005>.
- Türkmen, İ. and Kantarcı, A. (2007), “Effects of expanded perlite aggregate and different curing conditions on the physical and mechanical properties of self-compacting concrete”, *Build. Environ.*, **42**(6), 2378-2383. <https://doi.org/10.1016/j.buildenv.2006.06.002>.
- Verma, S.K., Bhadauria, S.S. and Akhtar, S. (2013), “Evaluating effect of chloride attack and concrete cover on the probability of corrosion”, *Front. Struct. Civil Eng.*, **7**, 379-390. <https://doi.org/10.1007/s11709-013-0223-9>.
- Wu, Z. (1979), “An approach to the recent trends of concrete science and technology”, *J. Chin Ceram. Soc.*, **7**(3), 262-270. (in Chinese)
- Yan, X., Jiang, L., Guo, M., Chen, Y., Song, Z. and Bian, R. (2019), “Evaluation of sulfate resistance of slag contained concrete under steam curing”, *Constr. Build. Mater.*, **195**, 231-237. <https://doi.org/10.1016/j.conbuildmat.2018.11.073>.
- Yang, C.C. and Wang, L.C. (2004), “The diffusion characteristic of concrete with mineral admixtures between salt ponding test and accelerated chloride migration test”, *Mater. Chem. Phys.*, **85**(2-3), 266-272. <https://doi.org/10.1016/j.matchemphys.2003.12.025>.
- Zhang, P. and Li, Q. F. (2013), “Effect of silica fume on durability of concrete composites containing fly ash”, *Sci. Eng. Compos. Mater.*, **20**(1), 57-65. <https://doi.org/10.1515/secm-2012-0081>.
- Zhang, P. and Li, Q. F. (2014), “Freezing-thawing durability of fly ash concrete composites containing silica fume and polypropylene fiber”, *Proc. Inst. Mech. Eng., Part L: J. Mater.: Des. Appl.*, **228**(3), 241-246. <https://doi.org/10.1177/1464420713480984>.
- Zou, C., Long, G., Ma, C. and Xie, Y. (2018), “Effect of subsequent curing on surface permeability and compressive strength of steam-cured concrete”, *Constr. Build. Mater.*, **188**, 424-432. <https://doi.org/10.1016/j.conbuildmat.2018.08.076>.
- Zou, C., Long, G., Xie, Y., He, J., Ma, C. and Zeng, X. (2019), “Evolution of multi-scale pore structure of concrete during steam-curing process”, *Microporous Mesoporous Mater.*, **288**(1), 109566. <https://doi.org/10.1016/j.micromeso.2019.109566>.